

## Hydrodynamical evolution in heavy-ion collisions and pp scatterings

K. WERNER<sup>(1)</sup>, IU. KARPENKO<sup>(2)</sup> and T. PIEROG<sup>(3)</sup>

<sup>(1)</sup> *SUBATECH, University of Nantes, IN2P3/CNRS-EMN - Nantes, France*

<sup>(2)</sup> *Bogolyubov Institute for Theoretical Physics - Kiev 143, 03680, Ukraine*

<sup>(3)</sup> *Karlsruhe Institute of Technology (KIT), Campus North, Institut für Kernphysik Karlsruhe, Germany*

(ricevuto il 10 Dicembre 2010; approvato il 23 Dicembre 2010; pubblicato online il 30 Marzo 2011)

**Summary.** — We discuss recent developments in the EPOS approach, concerning an event-by-event treatment of the hydrodynamical evolution in heavy-ion collisions and also high-multiplicity pp scatterings at the LHC. The initial conditions are flux tubes, which are formed following elementary (multiple) scatterings, both soft and hard ones.

PACS 25.75.-q – Relativistic heavy-ion collisions.

EPOS is a multiple scattering model in the spirit of the Gribov-Regge approach [1]. Here, one does not mean simply multiple hard scatterings, the elementary processes correspond to complete parton ladders, which means hard scatterings plus initial state radiation. In this case, an elementary process carries an important fraction of the available energy, and therefore we treat very carefully the question of energy sharing in the multiple scattering process. Open and closed ladders have to be considered, see fig. 1, in order to have a consistent quantum-mechanical treatment. The corresponding graphs are squared, and we employ cutting rule techniques and Markov chains to obtain finally partial cross sections. The cut parton ladders are identified with longitudinal color fields or flux tubes, treated via relativistic string theory.

In case of very high-energy pp collisions (at the LHC) or heavy-ion scatterings already at RHIC, many flux tubes overlap and produce high-energy densities. Let us consider the energy density at an early time in a Au-Au scattering at RHIC, as obtained from an EPOS simulation [1]. In fig. 2, we plot the energy density at different values of space-time rapidity  $\eta_s$ , as a function of the transverse coordinates  $x$  and  $y$ . We observe a very bumpy structure concerning the  $x$ - $y$  dependence, whereas the variation with  $\eta_s$  is small. There are in particular peaks in the  $x$ - $y$  plane, which show up at the same position at different values of  $\eta_s$ . So we have sub-flux-tubes which exhibit a long-range structure in the longitudinal variable  $\eta_s$ . In fig. 2, we clearly identify several sub-flux-tubes, with a typical width of the order of a fermi. This is exactly the width we obtain if we

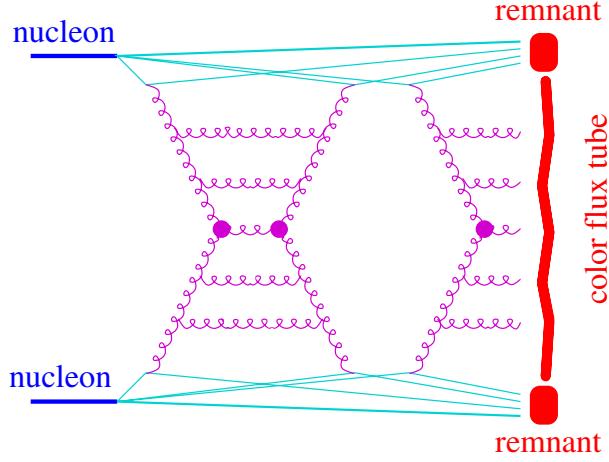


Fig. 1. – Multiple scattering diagram in EPOS.

compute the initial energy density in proton-proton scattering at the LHC. This means, if a hydrodynamic treatment is justified for Au-Au collisions at RHIC, it is equally justified for pp scattering at the LHC, provided the energy densities are high enough, which seems to be the case.

We are therefore going to employ a new tool for treating very high-energy hadronic interactions including a hydrodynamic evolution (even in pp), based on the following features (see [1]):

- initial conditions obtained from a flux tube approach compatible with the string model used for many years for elementary collisions (electron-positron, proton-proton), and the color glass condensate picture;
- consideration of the possibility to have a (moderate) initial collective transverse flow;

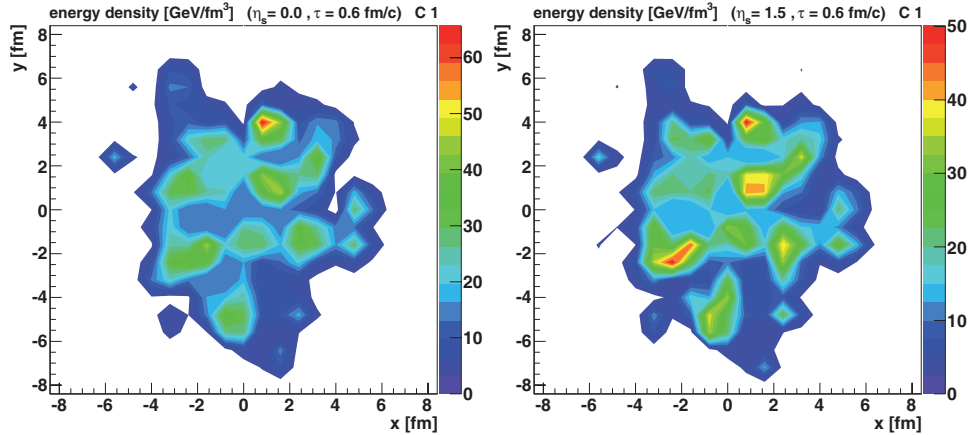


Fig. 2. – Energy density in central Au-Au scattering at 200 GeV.

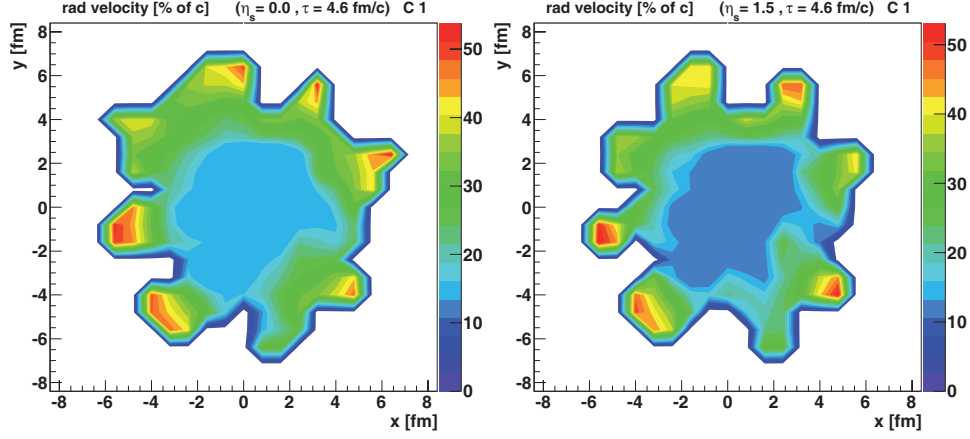


Fig. 3. – Radial flow velocity at a proper time  $\tau = 4.6 \text{ fm}/c$ , at a space-time rapidities  $\eta_s = 0$  and  $\eta_s = 1.5$ .

- event-by-event procedure, taking into account the highly irregular space structure of single events, being experimentally visible via the so-called ridge structures in two-particle correlations;
- core-corona separation, considering the fact that only a part of the matter thermalizes;
- use of an efficient code for solving the hydrodynamic equations in 3+1 dimensions, including the conservation of baryon number, strangeness, and electric charge;
- employment of a realistic equation of state, compatible with lattice gauge results, with a crossover transition from the hadronic to the plasma phase;
- use of a complete hadron resonance table, making our calculations compatible with the results from statistical models;
- hadronic cascade procedure after hadronization from the thermal system at an early stage.

In ref. [1], we test the approach by investigating all soft observables of heavy ion physics, in case of Au-Au scattering at 200 GeV. Here, we are going to discuss some selected (and interesting) topics. In fig. 2, we see a complicated structure of the initial energy density in the transverse plane, but this structure is longitudinally translational invariant (same structure at different values of  $\eta_s$ ). The equations of hydrodynamics preserve this translational invariance, and transport it to different quantities, as the radial flow, see fig. 3. As a consequence, particles emitted from different longitudinal positions get the same transverse boost, when their emission points correspond to the azimuthal angle of a common flow peak position. And since longitudinal coordinate and (pseudo)rapidity are correlated, one finally obtains a strong  $\Delta\eta$ - $\Delta\phi$  correlation, as seen in fig. 4, where we plot the dihadron correlation  $dN/d\Delta\eta d\Delta\phi$ , with  $\Delta\eta$  and  $\Delta\phi$  being, respectively, the difference in pseudorapidity and azimuthal angle of a pair of particles. Here, we consider trigger particles with transverse momenta between 3 and 4 GeV/c,

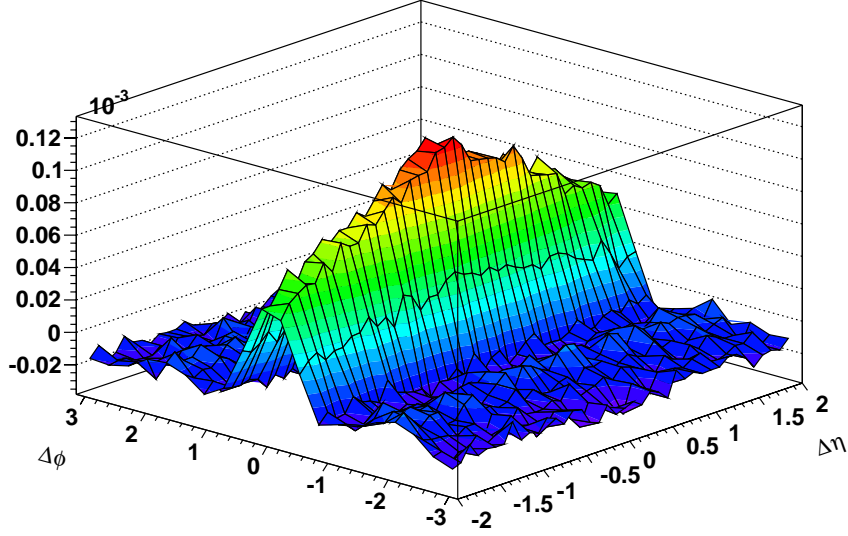


Fig. 4. – Dihadron  $\Delta\eta$ - $\Delta\phi$  correlation in a central Au-Au collision at 200 GeV, as obtained from an event-by-event treatment of the hydrodynamical evolution based on random flux tube initial conditions. Trigger particles have transverse momenta between 3 and 4 GeV/ $c$ , and associated particles have transverse momenta between 2 GeV/ $c$  and the  $p_t$  of the trigger.

and associated particles with transverse momenta between 2 GeV/ $c$  and the  $p_t$  of the trigger, in central Au-Au collisions at 200 GeV. Our ridge is very similar to the structure observed by the STAR Collaboration [2].

Let us consider proton-proton scattering now, for details see [3]. In fig. 5, we show as an example the energy density at  $\tau = 0.6$  fm/ $c$  for a high-multiplicity pp collision at 900 GeV, where high multiplicity here refers to a plateau height  $dn/d\eta$  of 12.9, which is

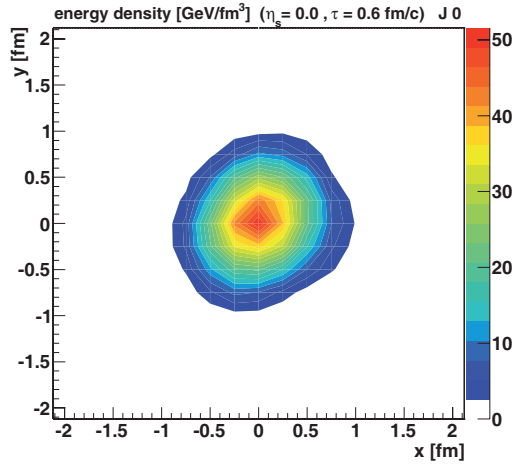


Fig. 5. – Initial energy density in a high-multiplicity pp collision ( $dn/d\eta = 12.9$ ) at 900 GeV, at a space-time rapidity  $\eta_s = 0$ .

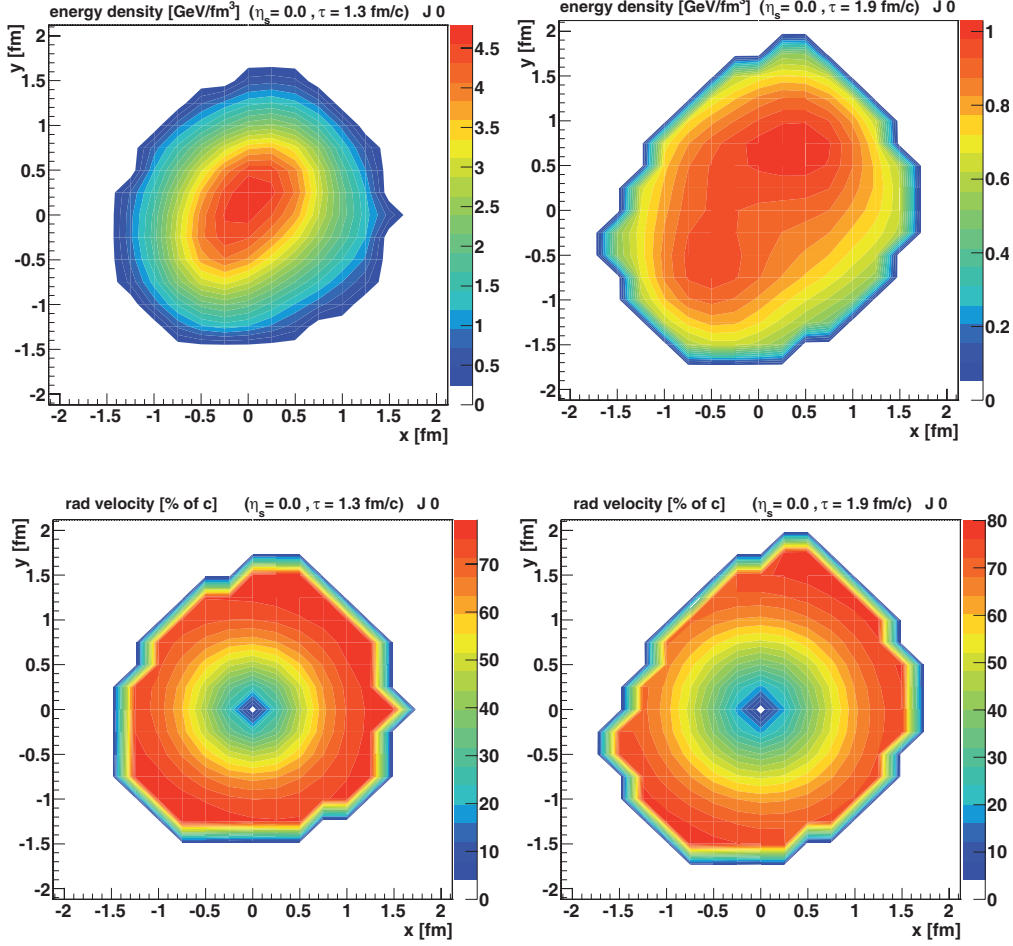


Fig. 6. – Energy density (upper panel) and radial flow velocity (lower panel) for a high multiplicity pp collision ( $dn/d\eta = 12.9$ ) at 900 GeV, at proper times  $\tau = 1.3$  fm/c (left) and  $\tau = 1.9$  fm/c (right), at a space-time rapidity  $\eta_s = 0$ .

more than 3 times the average. We see a maximum energy density of about  $50 \text{ GeV/fm}^3$ , which indeed corresponds to the energy densities observed in central gold-gold collisions at 200 GeV. Even more, comparing with the spiky single event results for gold-gold in [1], our pp distribution corresponds to one (of many) spikes in gold-gold at 200 GeV, which means a hydrodynamic treatment for pp is as good (or bad) as for gold-gold at 200 GeV.

Starting from the flux tube initial condition, the system expands very rapidly. In fig. 6, we show the hydrodynamic evolution of the event corresponding to the initial energy density of fig. 5, which can be considered as a typical example, with similar observations being true for randomly chosen events of this multiplicity ( $dn/d\eta = 12.9$ ). We see that the system evolves immediately also transversely, the energy density drops very quickly. A very large transverse flow develops typically around 70% of the velocity of light. This will have measurable consequences.

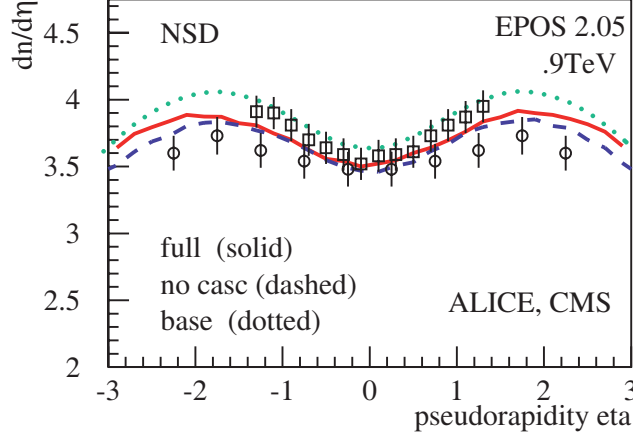


Fig. 7. – Pseudorapidity distributions in pp scattering at 900 GeV, compared to data (points). We show the full calculation (solid line), a calculation without hadronic cascade (dashed), and a calculation without hydro and without cascade (dotted).

We first check some elementary distributions. We only consider 900 GeV, for higher energies some reconsideration of our screening procedures will be necessary (work in progress). As usual we work with the event-by-event mode, and hydrodynamics is only employed for high-density areas (core-corona separation).

In the following we will compare three different scenarios:

full: the full calculations, including hydro evolution and hadronic cascade;

no casc: calculation without hadronic cascade;

base: calculation without hydro and without cascade.

We will compare the corresponding calculations with experimental data, for pp scattering at 900 GeV.

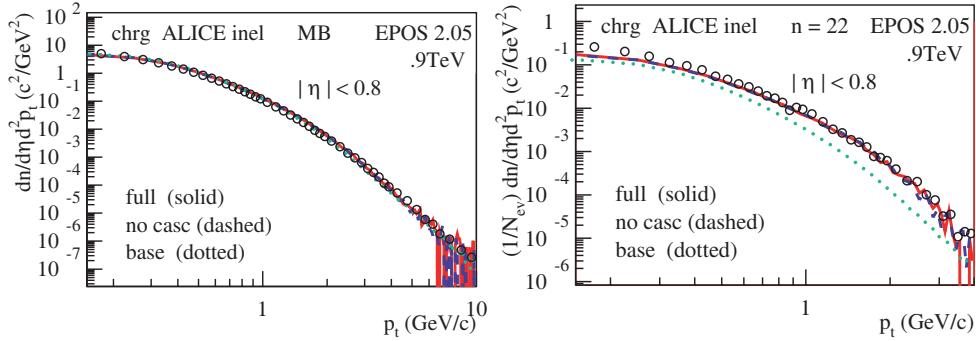


Fig. 8. – Transverse momentum distributions in pp scattering at 900 GeV, for minimum bias events (left panel) and high-multiplicity events ( $n = 22$ , right panel), compared to data (points). We show the full calculations (solid lines), a calculation without hadronic cascade (dashed), and a calculation without hydro and without cascade (dotted).

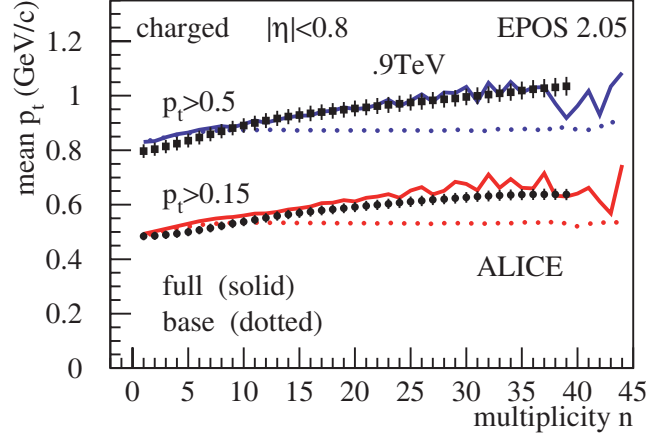


Fig. 9. – Mean transverse momentum as a function of the charged multiplicity in pp scattering at 900 GeV, compared to data (points). We show the full calculation (solid line), and a calculation without hydro and without cascade (dotted).

In fig. 7, we show pseudorapidity distributions of charged particles, compared to data from CMS [4] and ALICE [5, 6]. The three scenarios do not differ very much, and agree roughly with the data.

We then investigate transverse momentum distributions. For minimum bias events, there is again little difference for the three scenarios (all of them reproduce the data within 20%), as seen in the left panel of fig. 8. The situation changes drastically, when we consider high-multiplicity events, see the right panel of fig. 8, where  $n = 22$  refers to the charged particle multiplicity in the pseudorapidity range  $|\eta| < 0.8$ . Here the base calculation (without hydro) underestimates the data by a factor of three, whereas the full calculation gets close to the data. This is a very typical behavior of collective flow: the distributions get harder at intermediate values of  $p_t$  (around 1–4 GeV/c).

In fig. 9, we plot the mean transverse momentum as a function of the charged multiplicity, compared to data from ALICE [6]. The increase of the mean  $p_t$  with multiplicity is in our approach related to collective flow: with increasing multiplicity one gets higher initial energy densities, and more collective flow can develop. The data are therefore compatible with our flow picture, but for a real proof one needs at least in addition the mean  $p_t$  behavior of heavier particles (protons, lambdas, or even heavier), since the effect gets bigger with increasing mass.

To summarize: after having recently introduced a sophisticated approach of hydrodynamic expansion based on flux tube initial conditions for Au-Au collisions at RHIC, we now employ exactly the same picture to pp scattering at 900 GeV, which is in particular justified for high-multiplicity events. Comparing with experimental data seems to support this approach.

## REFERENCES

- [1] WERNER K., KARPENKO I.U., PIEROG T., BLEICHER M. and MIKHAILOV K., *Phys. Rev. C*, **82** (2010) 044904.
- [2] ABELEV B. *et al.* (STAR COLLABORATION), *Phys. Rev. C*, **80** (2009) 64192.

- [3] WERNER K., KARPENKO I.U., PIEROG T., BLEICHER M. and MIKHAILOV K., arXiv:1010.0400, submitted to *Phys. Rev. C*.
- [4] CMS COLLABORATION, *J. High Energy Phys.*, **02** (2010) 041.
- [5] ALICE COLLABORATION, arXiv:1007.0719.
- [6] AAMODT K. *et al.* (ALICE COLLABORATION), *Eur. Phys. J. C*, **68** (2010) 89.